Published in final edited form as:

Biochim Biophys Acta Mol Basis Dis. 2020 March 01; 1866(3): 165620. doi:10.1016/j.bbadis.2019.165620.

Genes of the cGMP-PKG-Ca^{2+} signaling pathway are alternatively spliced in cardiomyopathy: Role of RBFOX2

Xianxiu Wan[1], **KarryAnne Belanger**[2], **Steven G Widen**[2], **Muge N Kuyumcu-Martinez**[2,+], **Nisha J Garg**[1,3,+]

[1]Department of Microbiology & Immunology, University of Texas Medical Branch, Galveston, 77555-1070, Texas

[2]Department of Biochemistry and Molecular Biology, University of Texas Medical Branch, Galveston, 77555, Texas

[3]Institute for Human Infections and Immunity, University of Texas Medical Branch, Galveston, 77555 Texas

Abstract

Aberrations in the cGMP-PKG-Ca^{2+} pathway are implicated in cardiovascular complications of diverse etiologies, though involved molecular mechanisms are not understood. We performed RNA-Seq analysis to profile global changes in gene expression and exon splicing in Chagas disease (ChD) murine myocardium. Ingenuity-Pathway-Analysis of transcriptome dataset identified 26 differentially expressed genes associated with increased mobilization and cellular levels of Ca^{2+} in ChD hearts. Mixture-of-isoforms and Enrichr KEGG pathway analyses of the RNA-Seq datasets from ChD (this study) and diabetic (previous study) murine hearts identified alternative splicing (AS) in eleven genes (*Arhgef10*, *Atp2b1*, *Atp2a3*, *Cacna1c*, *Itpr1*, *Mef2a*, *Mef2d*, *Pde2a*, *Plcb1*, *Plcb4*, *and Ppp1r12a*) of the cGMP-PKG-Ca^{2+} pathway in diseased hearts. AS of these genes was validated by an exon exclusion-inclusion assay. Further, *Arhgef10*, *Atp2b1*, *Mef2a*, *Mef2d*, *Plcb1*, and *Ppp1r12a* genes consisted RBFOX2 (RNA-binding protein) binding-site clusters, determined by analyzing the RBFOX2 CLIP-Seq dataset. H9c2 rat heart cells transfected with *Rbfox2* (vs. scrambled) siRNA confirmed that expression of *Rbfox2* is essential for proper exon splicing of genes of the cGMP-PKG-Ca^{2+} pathway. We conclude that changes in gene expression may influence the Ca^{2+} mobilization pathway in ChD, and AS impacts the genes involved in cGMP/PKG/Ca^{2+} signaling pathway in ChD and diabetes. Our findings suggest that ChD patients with diabetes may be at increased risk of cardiomyopathy and heart failure and

[+]**Corresponding authors:** Nisha J Garg, PhD MBA, nigarg@utmb.edu, O: 409-747-6865, Muge N Kuyumcu-Martinez, PhD, nmmartin@utmb.edu, O: (409) 772-3228.

Author contribution: NJG and MKM conceived the study, provided financial support, and wrote the manuscript. XW and KKB have designed and performed the experiments, analyzed data, and confirmed the accuracy of data presented in the manuscript. XXW participated in writing the manuscript. KKB helped edit the manuscript. SGW performed all the next generation sequencing studies and computational analysis and contributed to discussion. All authors have read and approved the manuscript to be published.

Disclosure: The funders had no role in study design, data collection and analysis, decision to publish or preparation of the paper.

Competing interests: All authors declare that they have no financial or other competing interests.

provide novel ways to restore cGMP-PKG regulated signaling networks via correcting splicing patterns of key factors using oligonucleotide-based therapies for the treatment of cardiovascular complications.

Keywords

Cardiomyopathy; Alternative splicing; RNA-binding protein RBFOX2; Protein kinase G; Calcium homeostasis; Chagas; Diabetes

INTRODUCTION

Diabetes mellitus (DM) is a group of metabolic diseases characterized by insulin insufficiency and high blood glucose levels. Several studies have established that adiposity exacerbates the metabolic disorder and insulin insufficiency and is the main source of pathophysiological outcomes in DM (reviewed in [1–3]). DM, regardless of etiology, can adversely affect the cardiac muscle cells, causing alterations to cellular structure, metabolism, calcium signaling, and induction of hypertrophy and fibrosis independent of hypertension and atherosclerosis [4–6]. Cardiovascular complications of DM are the leading cause of death among diabetic patients [4, 7].

Chagas disease (ChD) is caused by *Trypanosoma cruzi* (*T. cruzi* or *Tc*). ChD is a major health concern in Latin America, and an emerging infectious disease in the United States [8, 9]. Up to 30% of the infected individuals develop dilated cardiomyopathy presented with ventricular dilation, arrhythmias, conduction disturbances, and intra-cavity thrombi that lead to heart failure and sudden death [10]. ChD costs approximately eight billion US dollars per year in healthcare costs and in loss of productivity [11]. Recent studies have shown that parasite persistence in adipose tissue and alterations in insulin release are common features of Chagas disease [12, 13]. Whether adiposity with impaired glucose and insulin homeostasis that are the pathophysiologic features of DM exacerbate the cardiac complications in ChD remains incompletely understood.

The cyclic GMP (cGMP) dependent protein kinase G (PKG) plays a key role in maintaining cardiac homeostasis. In the heart, nitric oxide and natriuretic peptides signal cGMP formation, and cGMP serves as secondary messenger in activation of PKG [14]. PKG phosphorylates several proteins that play an essential role in regulation of Ca^{2+} signaling, contraction and relaxation of cardiac myocytes and vascular smooth muscle cells (VSMC), and in inhibiting inflammation and reducing oxidative stress [15]. Activation of cGMP-PKG signaling through inhibition of cGMP hydrolysis by phosphodiesterases was cardioprotective and ameliorated cardiovascular complications in ChD [16] and diabetic [16–19] rodent models. Detailed mechanisms responsible for dysregulation of cGMP-PKG in the heart exposed to diverse pathological stimuli are not known.

Alternative splicing (AS) is a mechanism by which different forms of mature mRNAs are generated from a single gene. In this process, particular exons of a gene may be incorporated or excluded from the final mRNA product [20]. AS is an essential mechanism that increases proteome diversity [21]. Proper regulation of AS is critical for cardiac cell function, growth,

and development [21, 22]. AS is controlled by RNA-binding proteins (RBPs), which bind pre-mRNAs and control AS decisions via interacting with the splicing machinery.

The RBFOX2 family of RBPs is implicated in coordinated AS transitions during heart [22–24] and brain development [25, 26]. Recent studies have shown that *de novo* mutations in *RBFOX2* are associated with specific congenital heart defects [27]. Importantly, down regulation of *Rbfox2* in pressure overload induced heart failure contributed to aberrant AS patterns in the heart and conditional ablation of *Rbfox2* in mouse cardiomyocytes led to dilated cardiomyopathy [28]. We have shown that RBFOX2 splicing activity was repressed in diabetic hearts due to increased expression of a dominant negative spliced isoform of *Rbfox2* gene [29]. Importantly, changes in RBFOX2 splicing function altered the calcium homeostasis and proper expression of actin associated proteins leading to cardiomyocyte dysfunction [29].

In this study, we aimed to determine if splicing of exons in genes involved in the cGMP-PKG-Ca^{2+} pathway is disturbed in experimental ChD and DM models. We examined AS patterns of genes associated with cGMP-PKG-Ca^{2+} signaling pathway in ChD and diabetic mice. We also tested if RBFOX2 regulates AS of genes of the cGMP-PKG signaling pathway. Together, our results provide the first evidence for a common pathway of AS of critical genes associated with myocardial cGMP-PKG-Ca^{2+} signaling in ChD and diabetes models. Further studies will determine if DM exacerbates the AS of genes, and consequently the dysfunction of the cGMP-PKG-Ca^{2+} signaling pathway and severity of cardiomyopathy and heart failure in Chagas patients.

MATERIALS AND METHODS

Ethics statement

All animal experiments were performed by following the NIH guidelines for Care and Use of Experimental Animals, and in accordance with protocols approved by the Institutional Animal Care and Use Committee at the University of Texas Medical Branch, Galveston (Protocol numbers: 0805029 and 1101001).

Mice, parasites, and cell culture

C57BL/6 mice (males and females, six-weeks old) were purchased from Jackson Laboratory (Bar Harbor, ME). Mice (males) injected daily with 60 mg/kg of streptozotocin for five days offer an established model of DM [29], and this model was used in this study. As controls, mice were injected daily with citrate buffer for 5 days. OneTouch Ultra 2 Glucometer was used to determine the fasting blood glucose levels in streptozotocin-injected mice. Mice with blood glucose levels of >450 mg/dl were euthanized and left ventricle (LV) tissues were isolated for RNA extraction.

For Chagas disease, trypomastigotes of *T. cruzi* (SylvioX10/4 strain, ATCC 50823) were maintained and propagated by continuous *in vitro* passage in C2C12 immortalized mouse myoblast cells (ATCC CRL-1772) as described previously [30]. Female mice were infected with *T. cruzi* (10,000 trypomastigotes/mouse, intraperitoneal) and euthanized at 150 days post-infection (pi). This is an established experimental model of ChD; infected mice develop

acute parasitemic phase for 7–40 days post-infection (pi) [10, 31], pathological changes associated with inflammatory infiltrate, oxidative stress, and fibrosis by 90 days pi [32], and left ventricular dysfunction is presented by 150 days pi [33]. Sera/plasma and tissue samples were stored at −80°C [34].

Embryonic rat heart-derived H9c2 cells (ATCC CRL1446) were maintained in Dulbecco's modified Eagle's medium (DMEM) supplemented with glutamine containing 10% heat-inactivated fetal bovine serum (FBS, Invitrogen, Carlsbad, CA) and penicillin/streptomycin solution (100-μg each antibiotic per ml, Corning, Corning, NY) at 37°C in a 5% CO_2 humidified incubator. H9c2 cells (2×10^5 per well in 12-well plates) were transfected in duplicate with 50 nM of *Rbfox2*-specific siRNA (s96620, Invitrogen) targeting exon 5 and exon 6 of *Rbfox2*. Cells transfected with scrambled siRNA (AM4611, Invitrogen) were used as controls. All transfections were performed by using the Neon Nucleofection system (Invitrogen), by following the protocol previously described by us [29]. Cell lysates were collected for RNA isolation.

High throughput RNA sequencing and statistical analysis

Heart tissue sections (10 mg/ml) from ChD, diabetic, and matched control mice ($n \geq 3$ per group per experiment) were suspended in TRIzol reagent (15596–018, Invitrogen). Total RNA was extracted and precipitated by chloroform/isopropanol/ethanol method. RNA concentration was determined by using the EPOCH microplate spectrophotometer (BioTek, Winooski, VT). RNA quality was determined by using a Bioanalyzer RNA 6000 Nano assay that detects the integrity of 18S and 28S rRNAs (Agilent Technologies, Santa Clara, CA).

Poly-A^+ RNA was enriched from total RNA (1 μg) by using oligo dT-attached magnetic beads. Bound RNA was fragmented by incubation at 94°C for 8 min in 19.5 μl of fragmentation buffer (Illumina, San Diego, CA). A TruSeq RNA Sample Preparation kit was employed for first and second strand synthesis, adapter ligation, and amplification of the library, as recommended by the manufacturer (Illumina). Library quality was evaluated on an Agilent DNA-1000 chip / Agilent 2100 Bioanalyzer. A TruSeq SBS kit v.3 (Illumina) was used to perform paired end 50 base sequencing on an Illumina HiSeq 1000 by following the protocols defined by the manufacturer. Sequencing was performed at the UTMB Next Generation Sequencing Core Facility and yielded ~100 million read pairs per sample.

Raw RNA-Seq reads were first aligned to the mouse mm9 and mm10 reference genomes (downloaded from the Illumina Inc. iGenomes database) by using STAR (version 2.4.0j) software [35] with default settings. To obtain the differential gene expression (DGE) data, the FeatureCounts function of the subread software program [36] was used with the mm10 mapped reads and the corresponding Illumina iGenome gene annotation file normalization and differential gene expression analysis were performed with Bioconductor DESeq2 software (version 1.20.0) [37]. Significant genes were called at an adjusted p-value of < 0.01. FDR adjusted p-values were then calculated by using the Benjamini-Hochberg procedure.

To identify the differentially regulated exons (i.e. AS isoforms) in Chagas disease, the RNA-Seq data of ChD (vs. control) hearts were probed by mixture-of-isoforms (MISO, version.

0.5.3) [38] analysis. Here, we used the reads mapped to reference mm9 to match the MISO annotations. The MISO was used with a cut-off of >10% splicing changes with the criteria that the statistical significance or Bayes factor is > 1, as we have described previously [24].

Genome-wide RBFOX2 binding sites were previously identified in human ES cells by CLIP-seq [43]. These datasets became available in March 2006 hg18 version of the genome browser and were used for identifying the RBFOX2-binding sites in genes that undergo AS changes in Chagas hearts.

Bioinformatics and network analysis

We used the Ingenuity Pathway Analysis (IPA) web-based application (Ingenuity Systems, Redwood city, CA) to integrate the gene expression dataset (fold change: |>1.2|, $p<0.01$), into defined networks and signaling pathways associated with ChD development [39, 40].

We performed gene ontology analysis of the differentially regulated exon datasets (fold change: |>1.2|, $p<0.01$) by using the Enrichr databases server (https://amp.pharm.mssm.edu/Enrichr/) to identify the KEGG mouse pathways affected by AS events in diseased (vs. control) hearts.

Exon inclusion/exclusion analysis

Heart tissues (10 mg/ml) or cell pellets (2×10^5 / 200 μl) were suspended in TRIzol, and total RNA was extracted and precipitated by chloroform/isopropanol/ethanol method. Total RNA was analyzed for quality ($OD_{260/280}$ ratio > 2.0) and quantity (OD_{260} of 1 = 40 μg/ml RNA) by using a NanoDrop ND-1000 spectrophotometer (Wilmington, DE). Purified RNA (1 μg) was added to a 20 μL reaction mix with AMV reverse transcriptase (15 units/μg, Life Biosciences, Boston, MA), 10 μM dNTPs, and oligo dT_{18} primer, and cDNA synthesis was carried out at 42°C for 1 h. Gene-specific PCR primers for mouse and rat were designed using Primer3 v.4.1.0 software to detect inclusion/exclusion of specific exons. All genes, target exons, and oligonucleotides are listed in Table S1. The PCR reaction was performed in a 20-μL reaction with 5 μl of cDNA template, 25 μM dNTPs, 100 ng of gene-specific forward and reverse primers, and 1 unit of Biolase Taq polymerase (Bioline, Memphis, TN). PCR conditions for each reaction were as following: 94°C, 45 sec; 59°C, 45 sec; and 72°C, 1 min for 25 or 27 cycles. PCR products were resolved on a 5% non-denaturing polyacrylamide gel and stained with ethidium bromide. The gel images were visualized and analyzed by using a Gel Doc XR Imaging system (BioRad, Hercules, CA) [29].

Gene expression

Total RNA was isolated from H9c2 cells transfected with *Rbfox2*-specific or scrambled siRNAs by TRIzol method and cDNA synthesis was carried out at 42°C for 1 h, as described above. The real time quantitative PCR was performed on an iCycler thermal cycler in a 20 μl reaction containing 1 μl cDNA, 10 μl SYBR green master mix (Bio-Rad), and 500 nM of oligonucleotide pairs for *Rbfox2* (exon 3–5) or *Gapdh* gene sequence. The thermal cycling conditions were as follows: denature at 95°C for 30 sec, anneal at 60°C for 30 sec, and then denature-anneal cycling 39 more times. Specific product amplification was confirmed in the melt curve analysis. The PCR base line subtracted curve fit model was applied for threshold

cycle (Ct), and mRNA level was calculated using iCycler iQ real-time detection system software (Bio-Rad). The C_t values of *Rbfox2* mRNAs were normalized to mean Ct values for the *Gapdh* housekeeping mRNA sequence, and the relative mRNA level of *Rbfox2* was calculated by $2^{-\Delta Ct}$ method, where ΔC_t represents the C_t (target) - C_t (reference) [33].

Western blotting

Heart tissues (tissue: buffer ratio, 1:10 w/v) or cell pellets (cell: buffer ratio, 1:10 v/v) were homogenized in RIPA buffer (9806, Cell Signaling, Danvers, MA). Homogenates were centrifuged at 10,000 × g and supernatants were used as protein lysates. Protein lysates (50 μg) were electrophoresed on a 4–15% Mini-Protein TGX gel by using a Mini-PROTEAN electrophoresis chamber (Bio-Rad), and proteins were transferred to PVDF membrane by using a Criterion Trans-Blot System (Bio-Rad). Membranes were blocked with 50 mM Tris-Cl (pH 7.5), 150 mM NaCl (TBS) containing 5% non-fat dry milk (NFDM), washed three times for 10 min each with TBS-0.1% Tween 20 (TBST), and incubated overnight at 4°C with anti-RBFOX2 antibody (1:1000, Abcam, ab57154) or for 1 h at room temperature with anti-GAPDH antibody (Cell signaling, 1:3000, 3683). Membranes were washed and incubated for 1 h with light chain-specific anti-mouse IgG-HRP (1:5000-dilution, 115-035-174, Jackson ImmunoResearch Laboratories, West Grove, PA) or HRP-conjugated anti-rabbit antibody (1:10,000 dilution, Southern Biotech, Birmingham, AL). Membranes were incubated with SuperSignal West Femto (Pierce 34096) substrate or Pierce ECL2 (P80196, Thermo Fisher Scientific), and chemiluminescent signal was imaged and analyzed by using an ImageQuant LAS4000 system (GE Healthcare, Pittsburgh, MA). Densitometry analysis of protein bands of interest was performed by using a Fluorchem HD2 Imaging System (Alpha-Innotech, San Leandro, CA), and normalized against murine GAPDH [41].

Statistical analysis

For murine studies, mice were randomly assigned to diverse groups (n=5 mice per group), all murine samples were analyzed in duplicate or more, and experiments were conducted twice. For *in vitro* studies, at least two biological replicates were analyzed in each experiment, and all experiments were conducted thrice using new batches of biological replicates. Data were analyzed by using GraphPad Prism software (version 7, La Jolla, CA), and presented as mean value ± standard deviation (SD). Student's *t* test (comparison of two groups) and one-way analysis of variance (ANOVA) with Tukey's post-hoc test (comparison of more than two groups) were employed to evaluate the statistical significance. Significance is annotated as *p<0.05, **p<0.01, and ***p<0.001 (treatment vs. control).

RESULTS

Genome-wide gene expression and alternative splicing changes in Chagas heart disease

The cGMP-PKG-Ca^{2+}pathway plays a crucial role in modulating cardiac homeostasis. We hypothesized that the genes associated with the cGMP-PKG-Ca^{2+} pathway are altered in cardiomyopathy. To address this, we employed RNA-Seq to examine the global changes in gene expression and alternative splicing (AS) in ChD (vs. control) hearts of mice. Our data showed that 794 genes were differentially expressed at the mRNA level in ChD (vs. control) mice (fold change ≥ |1.2|, adjusted p value ≤ 0.01, Table S2). Of these, 96.2% (753 out of

783) of the genes were up regulated and 3.8% (30 out of 783) of the genes were down regulated at the mRNA level in ChD (vs. control) hearts (Figure 1A and Table S2). IPA analysis of the transcriptome dataset identified twenty-six target genes associated with mobilization and cellular levels of Ca^{2+} were differentially regulated in ChD (vs. control) hearts (z score: 1.926–1.980, p value: 5.84E-07 to 2.46E-02, Figure 1B). *Atp2a3* gene that encodes SERCA Ca^{2+} ATPase intracellular pump involved in catalysis of ATP hydrolysis coupled with translocation of Ca^{2+} from cytosol to sarcoplasmic reticulum lumen was also differentially expressed in ChD (vs. control) hearts (Table S2).

Next, we performed MISO analysis of the RNA-Seq dataset to examine alternative splicing changes in the ChD (vs. control) hearts. Based on the criteria that percent splicing change is >10% and the statistical significance Bayes factor is >1, we identified 210 cassette exon-splicing changes in ChD (vs. control) hearts (Table S3). Of these, 64.7% (136 out of 210) of the cassette exons were more included and 35.3% (74 out of 210) of the cassette exons were more excluded in ChD (vs. control) hearts (Figure 1C). To determine the biological consequences of these alternative splicing changes, we performed KEGG mouse pathway analysis by using the Enrichr server. In the chronic ChD mouse heart, top gene ontology categories affected by AS included the cGMP-PKG-Ca^{2+} signaling pathways (Figure 1D). Together, the results presented in Figure 1, Table S2, and Table S3 based on RNA-Seq analysis suggest that a) the genes involved in regulating Ca^{2+} mobilization and cellular homeostasis are differentially expressed, and b) the genes associated with the cGMP-PKG-Ca^{2+} signaling pathway undergo alternative splicing in Chagas disease hearts.

AS sites in genes associated with cGMP-PKG-Ca^{2+} signaling pathway in Chagas and DM models of heart disease

Focusing on the genes associated with cGMP-PKG-Ca^{2+} signaling pathway, we manually analyzed the differential AS dataset of ChD (Table S3) mice. We also used our previously published MISO dataset from DM mice [24, 29]. We identified five (*Arhgef10*, *Atp2b1*, *Atp2a3*, *Mef2a*, *Plcb1*) and eight (*Atp2b1*, *Cacna1c*, *Itpr1*, *Mef2a*, *Mef2d*, *Plcb4*, *Pde2a*) critical hubs within the cGMP-PKG-Ca^{2+} associated pathway that were alternatively spliced in ChD and DM mice, respectively (Table 1). The Genome browser images of the number of RNA-Seq reads mapped to the specific alternative exons in the genes associated with cGMP-PKG-Ca^{2+} pathway in ChD and DM hearts (vs. matched controls) are shown in Figure 2 and Figure 3. Two genes, *Atp2b1* (encodes for plasma membrane Ca^{2+} transporting ATPase 1 (PMCA1)) and *Mef2a* isoform of myocyte enhancer factor 2a (encodes Ca^{2+} sensitive DNA-binding transcription factor), were alternatively spliced in both ChD and DM mice. ChD murine hearts exhibited more exclusion of *Atp2b1* exon 5 and exon 21 and *Mef2a exon 9* (Figure 2A–2C) similar to DM murine hearts that also exhibited more exclusion of *Atp2b1 exon 21* and *Mef2a exon 9*, as reported in our previous studies [24, 29]. Other genes that were alternatively spliced in ChD (but not in DM) mice included *Atp2a3* which encodes for sarcoplasmic/endoplasmic reticulum associated Ca^{2+}-transporting ATPase 3 (SERCA3); *Arhgef10* for Rho-GEF10 that senses Ca^{2+} level and regulates smooth muscle relaxation; and *Plcb1* for phospholipase C beta that catalyzes the formation of inositol triphosphate (IP3) (Table 1). The *Atp2a3 Arhgef10*, and *Plcb1* were more excluded of exon 21, exon 9, and exon 32, respectively, in ChD (vs. control) hearts (Figure 2D–2F).

The genes that were alternatively spliced in DM-specific manner included *Cacna1c* for alpha 1 subunit of the voltage-dependent L-type calcium channel that mediates influx of Ca^{2+} ion into the cell upon membrane polarization; *Itpr* that encodes the intracellular IP3-stimulated receptor to modulate Ca^{2+} release from endoplasmic reticulum; *Ppp1r12a* for the myosin protein phosphatase 1 regulator that controls actin-myosin interaction downstream of GTP-RhoA; and *Pde2a* (phosphodiesterase 2a) that is a critical regulator of cGMP-to-cAMP cross-talk and cyclic nucleotide actions in cardiomyocyte microdomains (Table 1). Our data suggested more exclusion of *Cacna1c* exon 21 and 22, *Itpr* exon 15, *Ppp1r12a* exon 13, and *Pde2a* exon 2 in DM hearts compared to matched controls (Figure 3A–3D). *Mef2d* (an isoform of *Mef2*) exon 9 and *Plcb4* (phospholipase C beta 4) exon 13 were also more excluded in DM (vs. control) murine hearts (Figure 3E & 3F).

Together, the results presented in Figure 2 and Figure 3 show that eleven genes (*Arhgef10, Atp2b1, Atp2a3, Cacna1c, Itpr1, Mef2a, Mef2d, Pde2a, Plcb1, Plcb4, Ppp1r12a*) associated with cGMP-PKG-Ca^{2+} signaling pathway that encode for enzymes, calcium channels, and transcription factors with important roles in the cardiovascular system undergo alternative splicing in ChD and/or diabetic murine hearts, based on gene expression and alternative spliced variant analyses. It is predicted that exclusion of the specific exons will remove parts of the protein coding regions and may influence protein function.

Validation of AS of genes associated with cGMP-PKG-Ca^{2+} signaling pathway in Chagas and DM models of heart disease

Next, we validated the extent of AS of the selected genes of the cGMP-PKG-Ca^{2+} pathway in ChD and DM (vs. control) mice. For this, we utilized total RNA isolated from heart tissue of a new batch of mice and employed a semi-quantitative RT-PCR based inclusion/exclusion assay. In Figure 4, representative gel image from three mice per group demonstrating inclusion (+E) and exclusion (−E) of an exon in normal and ChD hearts are presented at top, and densitometry of percent inclusion of an exon evaluated in two separate experiments (total: six mice) is presented as bar graph below the gel image. These data showed that exon 21 and exon 5 of *Atp2b1*, exon 21 of *Atp2a3*, and exon 9 of *Mef2a* were excluded by more than 55%, 58%, 48%, and 14%, respectively, in ChD (vs. control) mice (Figure 4A–4D, p value < 0.05–0.001). These findings were consistent with our RNA-Seq analysis that identified increased exclusion of the select exons in *Atp2b1*, *Atp2a3*, and *Mef2a* genes (compare Figure 2A–2D with Figure 4A–4D). We did not detect a significant change in the inclusion/exclusion of exon 2 in *Pde2a*, exon 9 in *Arhgef10*, and exon 32 in *Plcb1* mRNAs in ChD (vs. control) mouse hearts by the semi-quantitative RT-PCR approach (Figure 4E–4G) as was noted by MISO analysis.

Likewise, semi-quantitative RT-PCR analysis of DM murine hearts showed that exon 22 of *Cacna1c*, exon 2 of *Pde2a*, *and* exon 9 of *Mef2d* were more excluded by 6%, 51.5%, and 41.2% respectively, in DM (vs. control) murine hearts (Figure 5A–5C, p value < 0.05–0.001). We have also demonstrated increased exclusion of exon 21 in *Atp2b1* and exon 9 in *Mef2a* in DM murine hearts previously [24, 29]. Exon 13 of *Ppp1r12a* was more included by 18.1% in DM (vs. control) murine hearts (Figure 5D, $p<0.05$).

Together, the results presented in Figure 4 and Figure 5 confirm the findings of RNA-Seq and AS analysis, and demonstrate that *Atp2b1*, *Atp2a3*, *Mef2a*, *Pde2a*, *Mef2d*, and *Ppp1r12a* genes of the cGMP-PKG pathway associated calcium channels undergo AS in the ChD and/or diabetic murine hearts.

Role of RBFOX2 in regulating AS of genes of the cGMP-PKG-Ca^{2+} pathway

RBFOX2, a RNA-binding protein, is known to regulate AS during development of the heart [28, 42], and may also influence the gene function through AS in diseased heart. We have previously found that a dominant negative (DN) isoform of *Rbfox2* was increased in expression, and this DN *Rbfox2* isoform led to a decline in RBFOX2 splicing activity and served as a major regulator of genome wide AS changes in the diabetic hearts [29]. In this study, we have noted up to 2-fold decline in the gene expression of *Rbfox2* in ChD (vs control) murine hearts (data not shown). We, therefore, chose to investigate if changes in RBFOX2 level (and therefore its activity) influence the extent of AS of genes of the cGMP-PKG-Ca^{2+} pathway.

Genome-wide RBFOX2 target pre-mRNAs have been identified by using cross-linking immunoprecipitation followed by RNA sequencing (CLIP-seq) analysis of human embryonic stem (ES) cells [43]. We used this publicly available RBFOX2 CLIP-seq dataset to examine the presence of RBFOX2-binding clusters in the eleven genes of the cGMP-PKG-Ca^{2+} signaling pathway that were identified to undergo AS in ChD and/or DM murine hearts by KEGG pathway analysis of RNA-seq and AS data (Figure 2 & Figure 3) and semi-quantitative RT-PCR (Figure 4 & Figure 5). We identified several strong RBFOX2 binding site clusters in *Arhgef10*, *Atp2b1*, *Mef2a*, *Mef2d*, *Plcb1*, and *Ppp1r12a* genes (Figure 6A–6G). The RBFOX2-binding sites were clustered in positive strand (blue dots) of *Arhgef10*, *Mef2a*, and *Plcb1*, and in the negative strand (red dots) of *Atp2b1*, *Mef2d*, and *Ppp1r12a* genes. The RBFOX2-binding clusters were noted close to exons that were increased in exclusion in these genes, and were also noticed in other intronic and exonic regions of some of these genes (Figure 6). A few randomly distributed RBFOX2-binding sites were identified within the exonic and intronic regions of *Atp2a3*, *Cacna1c*, *Pde2a*, *and Plcb4* (Figure S1), thus, suggesting that RBFOX2 may not have high affinity binding within these pre-mRNAs.

To experimentally validate that RBFOX2 indeed regulates the AS patterns in the genes of the cGMP-PKG-Ca^{2+} pathway, we performed *Rbfox2* depletion studies in rat-heart-derived H9c2 cells. H9c2 cells were transfected with small interfering RNA (siRNA) to target *Rbfox2* or scrambled control siRNA. We first confirmed the knockdown of *Rbfox2* expression in transfected cells. Transfection with *Rbfox2*^{siRNA} resulted in 78.5% knockdown of *Rbfox2* mRNA level, determined by real time RT-qPCR (Figure 7A), and subsequently, RBFOX2 protein was undetectable in *Rbfox2*^{siRNA} transfected cells as compared to that noted in controls (Figure 7B). These data confirmed that *Rbfox2*^{siRNA} efficiently knocked down the mRNA and protein levels of RBFOX2 in H9c2 cells. Next, we determined the effect of *Rbfox2* knockdown on AS events in the genes of cGMP-PKG-Ca^{2+} pathway. We noted that the inclusion of exon 21 in *Atp2b1* and exon 9 in *Mef2a* were decreased by 88.9% and 87.9%, respectively, in cells transfected with *Rbfox2*^{siRNA} in comparison to those transfected with scrambled siRNA (Figure 7C & 7D). These results were in agreement with

the finding of RBFOX2-binding site clusters within the exonic region of *Atp2b1* and *Mef2a* (Figure 6C & 6D). The AS of *Atp2a3* exon 21 was not significantly changed in *Rbfox2*^{siRNA} transfected (vs. control) cells (Figure 7D), consistent with its lack of RBFOX2-binding sites (Figure S1). These results suggest that RBFOX2 is essential for proper exon splicing of some of the major genes associated with the cGMP-PKG-Ca^{2+} pathway, and aberrations in RBFOX2 levels (and/or activity) will likely influence the expression and activity of the cGMP-PKG-Ca^{2+} pathway in ChD and DM hearts.

A schematic presentation of our findings in this study is shown in Figure 8. We have found AS changes in the genes of the cGMP-PKG-Ca^{2+} signaling pathway in ChD and DM hearts. *Atp2b1*, and *Mef2a* were similarly mis-spliced in both ChD and DM hearts and were regulated by RBFOX2. *Cacna1c*, *Itpr*, *Ppp1r12a* were alternatively spliced in the heart of diabetic mice; and *Arhgef10* and *Atp2a3* were differentially spliced in the heart of ChD mice. The AS events can impact the function of the target genes [20, 21] and *T. cruzi* infection is linked to increased risk of diabetes in Chagas patients (reviewed in [44]). We, therefore, propose that DM can potentially exacerbate the AS-induced dysregulation of cGMP-PKG-Ca^{2+} pathway and the severity of cardiomyopathy and heart failure in Chagas disease.

DISCUSSION

In the heart, nitric oxide (NO) and atrial natriuretic peptides signal the guanylyl cyclase - dependent cGMP production and the latter activates PKG. PKG phosphorylates serine and threonine residues on many cellular proteins and is known to mediate the downstream effects in maintaining the force of contraction of cardiac myocytes [45] through regulating cytosolic free Ca^{2+} levels and sensitivity of muscle fibers to Ca^{2+} [46]. In turn, phosphodiesterases (PDE) hydrolyze cyclic nucleotides [47] and negatively regulate cardiac inotropy [48]. An observation of PDE's subcellular localization to myocyte z-bands [49] implies that they may exert their effects on cGMP/PKG signaling in a spatiotemporal manner and determine the functional outcomes in stressed hearts. Indeed, we have shown that the activity of PKG was decreased in ChD heart, and sildenafil treatment (inhibits PDE5) provided a powerful protective effect against LV dysfunction in ChD mice [16]. The beneficial effects of PDE5 inhibition were delivered through normalization of PKG activity, increase in overall antioxidant response and ROS scavenging capacity, and a decline in cardiac collagenosis, oxidative adducts, and inflammatory infiltrate in chronic ChD [16]. We showed that sildenafil treatment also controlled, at least partially, the ADP-coupled oxidative metabolism in ChD myocardium [16], a finding that was in alignment with the suggestion that NO-cGMP-PKG signaling may also occur in mitochondria and play a role in ischemic pre-conditioning and antioxidant cardioprotection [50], though the exact mechanism remains to be identified. Likewise, activation of cGMP-PKG signaling ameliorated the cardiovascular complications of diabetes and was cardioprotective in animal models [17–19].

In this study, we wanted to determine whether expression of the genes/proteins that respond to cGMP-PKG signaling to maintain cardiac inotropy is affected in diabetic and ChD hearts. For this, we have performed RNA-Seq analysis of ChD hearts in this study (Figure 1A &

1B, Table S1) and analyzed RNA-Seq data of DM hearts from published studies [24, 51]. The analysis of these datasets for global and specific changes in gene expression profile identified no major changes in the expression of the genes downstream of cGMP-PKG signaling. We mostly noted the genes involved in systemic inflammation were increased in expression in ChD hearts; and these molecules were predicted to influence the Ca^{2+} mobilization and cytosolic Ca^{2+} concentration in cardiomyocytes during chronic ChD development (Figure 1B). Indeed, systemic inflammation and oxidative stress, routinely noted in humans and experimental models of ChD (reviewed in [10, 52]) and DM [53], can result in decreased bioavailability of NO through multiple mechanisms and thereby reduce the cGMP-PKG activation. We also noted in ChD hearts the increased expression of *S100a4* that encodes a Ca^{2+} binding protein and contributes to pathological cardiac remodeling [54] and decreased expression of *Nppb* (produces natriuretic peptide) that plays a key role in cardiovascular homeostasis through opposing signaling of cGMP-PKG and RAAS pathways [46, 55]. These findings allow us to propose that changes in gene expression primarily influence the events upstream of cGMP-PKG-Ca^{2+} signaling pathway in heart disease.

Alternative splicing of the exons may not be detectable depending on the size of the exons or the abundance of these transcripts by traditional RT-PCR and Western blotting approaches; however, AS can result in the formation of transcripts that influence the stability, sensitivity, functionality and signaling capabilities of the proteins [20, 21]. Indeed, we have identified 917 AS changes in type 1 diabetic hearts previously [56], and identified 210 AS changes in ChD hearts by MISO analysis of the RNA-Seq datasets in this study (Figure 1C and Table S3). Importantly, MISO analysis of the RNA-Seq datasets followed by KEGG pathway analysis showed that AS changes affected the genes that encode for calcium channels and cGMP-PKG signaling related molecules in the heart tissue of experimental models of ChD and DM (Figure 1, Figure 2, and Figure 3); and these findings were confirmed by semi-quantitative RT-PCR based inclusion/exclusion assay (Figure 4 & Figure 5). Importantly, AS changes in these genes remove specific internal exons; and are expected to remove parts of functional protein domains in ChD and DM hearts and thereby influence the activity of the cGMP-PKG-Ca^{2+} pathway (Figure 8). The genes that exhibited AS of exons in both ChD and diabetic hearts encode for isoforms of plasma membrane Ca^{2+} ATPase (PMCA1), MEF2 and PLC-β, and are discussed in more detail here.

We have noted increased exclusion of exon 21 in *Atp2b1* in ChD (Figure 4) and DM [56] hearts. *Atp2b1* encodes for a rather large (134 kDA) protein named plasma membrane Ca^{2+} ATPase (PMCA1) that belongs to the family of P-type primary ion transport ATPases, and it functions to maintain intracellular calcium homeostasis. Briefly, when Ca^{2+} increases in the cytosol, it binds to calmodulin, and Ca^{2+}-calmodulin complex activates and signals PMCA to remove Ca^{2+} from the cytosol [57]. PMCA, in turn, can bind to PI (4, 5) P2, and inhibit its availability for IP_3 formation. Less IP_3 will then release less Ca^{2+} from the intracellular stores, thus diminishing the Ca^{2+} signal in cells [58]. Besides the significant role of PMCA-dependent Ca^{2+} mobilization in maintaining the muscle contraction and relaxation functions, genome-wide association studies have linked polymorphism in *Atp2b1* gene to blood pressure and hypertension in Japanese population [59]. Subsequently, AS was found to generate more than 20 variants of PMCA isoforms (reviewed in [57]). These variants differ in their cell-specific localization and regulatory characteristics. Others have provided

molecular evidence for the association between reduced expression of PMCA1 and increased blood pressure with age [60]. Thus, it is possible that splice variants of *Atp2b1* may affect protein function and thereby contribute to increased stiffness of the arteries and a decline in cardiac contractility that are the common features of cardiomyopathy of ChD and DM etiologies.

Members of the MEF2 protein family belong to MADS-box transcription factors involved in cardiac development from embryogenesis to adulthood [61, 62]. We have noted AS changes in genes encoding for MEF2A/MEF2D in ChD and DM hearts in this study. It has been shown that *Mef2a* knockdown results in severely damaged cardiomyocytes, significant dilatation of the right ventricle, and mitochondrial derangement associated with increased mortality within the first week after birth [63]. MEF2D mediated regulation of PI3K/AKT contributes to post-mitotic state of cardiomyocytes, and *Mef2d* depletion promoted fetal gene expression and neonatal cardiomyocyte proliferation [64]; though prolonged depletion of *Mef2d* resulted in cardiomyocytes' death [65]. Exon 9 of *Mef2* that was noted to be excluded in the heart tissue of ChD and DM mice makes up the beta domain of MEF2, which is important for its transcription function [66]. Thus, we predict that AS of *Mef2* isoforms may affect its transcription function and thereby contribute to adverse cardiac outcomes in DM and ChD, to be verified in future studies.

PLC-beta catalyzes hydrolysis of phosphatidylinositol 4,5-bisphosphate to form inositol 1, 4, 5-trisphosphate (IP_3) that stimulates IP3-dependent Ca^{2+} release and downstream events leading to muscle contraction. The strength and activity of PLC-beta are regulated by a number of kinases including PKG through phosphorylation of PLC-beta that blocks Ca^{2+} mobilization and supports muscle relaxation [67]. Our RNA-Seq data showed increased exclusion of *Plcb1* exon 32 and *Plcb4* exon 13 in ChD and DM hearts, respectively (Figure 2 & Figure 3). Though alternatively spliced isoforms of *Plcb* are indistinguishable at mRNA and antigen level, several alternative spliced variants of PLC-beta have been reported in humans, rats, and mice, and most of these differ in their C-terminal sequences (reviewed in [68]) and potentially play different roles in cellular processes. Exclusion of *Plcb4* exon 13 would remove a portion of the EF hand domain that binds Ca^{2+} and is necessary for its catalytic activity [69]. Thus, it is predicted that mis-splicing of *Plcb* would impact its binding to calcium and subsequently its enzymatic function in ChD and DM hearts.

Specific to DM hearts, *Cacna1c* encodes for a component of the L-type calcium channel, and exons 21 and 22 that were excluded from *Cacna1c* in DM mouse hearts (Figure 3 & Figure 5) encode for the trans-membrane region of the channel that is modulated by blockers such as 1, 4 dihydropyridine [70]. We propose that AS may, at least partially, contribute to decreased L-type calcium channel voltage currents noted in diabetic myocytes [71]. PDE2 is a phosphodiesterase that can hydrolyze both cGMP and cAMP and impact a wide variety of downstream signaling pathways. PDE2A is a known spliced variant of *PDE2* gene that is localized to the cytosol due to the lack of membrane binding domain [72], and its increased abundance may also influence the cGMP-PKG pathway in diabetic heart.

We have previously shown that RBFOX2 is a contributor to AS dysregulation in the diabetic heart [29]. Here we provide evidence that RBFOX2 regulates AS of genes associated with

the cGMP-PKG signaling pathways including essential calcium channels. Consistent with our findings here, RBFOX2 has a role in regulating calcium transients in primary cardiomyocytes [28]. Arrhythmias and cardiomyopathy are the common pathologic features of chronic diabetes and ChD. Thus, it is possible that AS changes in calcium channels mediated via RBFOX2 may contribute to cardiac contractility and rhythm abnormalities in both diabetic and ChD hearts, to be validated in future studies.

A growing body of literature from animal and human studies indicate that *T. cruzi* infection is associated with alterations in insulin release (reviewed in [44]). A relationship between *T. cruzi* infection and insulin resistance, particularly as it applies to adipocyte function, has also been noted in experimental models of ChD [73]. In humans, the endocrine pancreatic dysfunction with impaired glucose homeostasis was noted long before the ChD patients developed clinical symptoms of cardiomyopathy and heart failure [74–76]. Other studies have shown that Chagas patients with cardiac manifestations have significantly higher rates of diabetes and hyperglycemia than was noted in seropositive individuals with no clinical heart disease [77]. These studies point to the fact that *T. cruzi* infection-induced hypoinsulinemia or hyperglycemia will increase the risk of DM in Chagas patients. Our finding in this study suggest that DM can potentially increase the risk and severity of cardiomyopathy and heart failure in chronic ChD through exacerbating the AS-induced dysregulation of the cGMP-PKG-Ca^{2+} signaling pathway. This hypothesis needs to be verified in future studies.

In summary, we have shown that AS of genes associated with cGMP-PKG-Ca^{2+} signaling pathway is increased in ChD and DM. We found that genes that were similarly mis-spliced in ChD and DM hearts were regulated by RBFOX2 (Figure 8). Though *Atp2b1* and *Mef2a* were alternatively spliced in both diseases (Figure 8), *Cacna1c*, *Itpr*, *Ppp1r12a* were alternatively spliced in the heart of diabetic but not in ChD mice; and *Arhgef10* and *Atp2a3* were alternatively spliced in the heart of ChD but not in diabetic mice. These differences in AS patterns can be used to specifically target these genes using antisense oligonucleotides to correct their splicing and restore protein function in a disease-specific manner. The common targets affected in both heart diseases can be targeted for more general therapy options. Our findings also provide a molecular basis to explain why Chagas patients with DM may be at an increased risk of cardiomyopathy and heart failure.

Supplementary Material

Refer to Web version on PubMed Central for supplementary material.

Acknowledgements

This work was supported, in part, by grants from of the National Institutes of Health, National Institute of Allergy and Infectious Diseases (R01AI054578; R01AI136031) to NJG and National Heart Lung Blood Institute (1R01HL135031) to MKM. XW was the recipient of Jeane B Kempner Postdoctoral Fellowship, UTMB. We are thankful to Dr. Sunil Verma and Dr. Jun Cao for help in designing the primers for exclusion / inclusion assays.

LITERATURE CITED

[1]. Kubota T, Kubota N, Kadowaki T, Imbalanced insulin actions in obesity and type 2 diabetes: Keymouse models of insulin signaling pathway, Cell Metab 25(4) (2017) 797–810. [PubMed: 28380373]

[2]. Boles A, Kandimalla R, Reddy PH, Dynamics of diabetes and obesity: Epidemiological perspective, Biochim Biophys Acta Mol Basis Dis 1863(5) (2017) 1026–1036. [PubMed: 28130199]

[3]. Chillaron JJ, Flores Le-Roux JA, Benaiges D, Pedro-Botet J, Type 1 diabetes, metabolic syndrome and cardiovascular risk, Metabolism 63(2) (2014) 181–7. [PubMed: 24274980]

[4]. Ferrannini E, Cushman WC, Diabetes and hypertension: the bad companions, Lancet 380(9841) (2012) 601–10. [PubMed: 22883509]

[5]. Harcourt BE, Penfold SA, Forbes JM, Coming full circle in diabetes mellitus: from complications to initiation, Nat Rev Endocrinol 9(2) (2013) 113–23. [PubMed: 23296171]

[6]. Boudina S, Abel ED, Diabetic cardiomyopathy revisited, Circulation 115(25) (2007) 3213–23. [PubMed: 17592090]

[7]. Aneja A, Tang WH, Bansilal S, Garcia MJ, Farkouh ME, Diabetic cardiomyopathy: insights into pathogenesis, diagnostic challenges, and therapeutic options, Amer J Med 121(9) (2008) 748–57. [PubMed: 18724960]

[8]. Bern C, Kjos S, Yabsley MJ, Montgomery SP, *Trypanosoma cruzi* and Chagas' Disease in the United States, Clin Microbiol Rev 24(4) (2011) 655–81. [PubMed: 21976603]

[9]. Tanowitz HB, Weiss LM, Montgomery SP, Chagas disease has now gone global, PLoS Negl Trop Dis 5(4) (2011) e1136. [PubMed: 21572510]

[10]. Lopez M, Tanowitz HB, Garg NJ, Pathogenesis of chronic Chagas disease: macrophages, mitochondria, and oxidative stress, Curr Clin Microbiol Rep 5(1) (2018) 45–54. [PubMed: 29868332]

[11]. Lee BY, Bacon KM, Bottazzi ME, Hotez PJ, Global economic burden of Chagas disease: a computational simulation model, Lancet Infect Dis 13(4) (2013) 342–8. [PubMed: 23395248]

[12]. Ferreira AV, Segatto M, Menezes Z, Macedo AM, Gelape C, de Oliveira Andrade L, Nagajyothi F, Scherer PE, Teixeira MM, Tanowitz HB, Evidence for *Trypanosoma cruzi* in adipose tissue in human chronic Chagas disease, Microbes Infect 13(12–13) (2011) 1002–5. [PubMed: 21726660]

[13]. Nagajyothi F, Machado FS, Burleigh BA, Jelicks LA, Scherer PE, Mukherjee S, Lisanti MP, Weiss LM, Garg NJ, Tanowitz HB, Mechanisms of *Trypanosoma cruzi* persistence in Chagas disease, Cell Microbiol 14(5) (2012) 634–643. [PubMed: 22309180]

[14]. Hofmann F, A concise discussion of the regulatory role of cGMP kinase I in cardiac physiology and pathology, Basic Res Cardiol 113(4) (2018) 31. [PubMed: 29934662]

[15]. Rainer PP, Kass DA, Old dog, new tricks: novel cardiac targets and stress regulation by protein kinase G, Cardiovasc Res 111(2) (2016) 154–62. [PubMed: 27297890]

[16]. Wen JJ, Wan X, Thacker J, Garg NJ, Chemotherapeutic efficacy of phosphodiesterase inhibitors in Chagas cardiomyopathy, JACC Basic Transl Sci 1(4) (2016) 235–250. [PubMed: 27747306]

[17]. Matyas C, Nemeth BT, Olah A, Torok M, Ruppert M, Kellermayer D, Barta BA, Szabo G, Kokeny G, Horvath EM, Bodi B, Papp Z, Merkely B, Radovits T, Prevention of the development of heart failure with preserved ejection fraction by the phosphodiesterase-5A inhibitor vardenafil in rats with type 2 diabetes, Eur J Heart Fail 19(3) (2017) 326–336. [PubMed: 27995696]

[18]. Kovacs A, Alogna A, Post H, Hamdani N, Is enhancing cGMP-PKG signalling a promising therapeutic target for heart failure with preserved ejection fraction?, Neth Heart J 24(4) (2016) 268–74. [PubMed: 26924822]

[19]. Das A, Durrant D, Salloum FN, Xi L, Kukreja RC, PDE5 inhibitors as therapeutics for heart disease, diabetes and cancer, Pharmacol Therapeut 147 (2015) 12–21.

[20]. Baralle FE, Giudice J, Alternative splicing as a regulator of development and tissue identity, Nat Rev Mol Cell Biol 18(7) (2017) 437–451. [PubMed: 28488700]

[21]. van den Hoogenhof MM, Pinto YM, Creemers EE, RNA splicing: Regulation and dysregulation in the heart, Circ Res 118(3) (2016) 454–68. [PubMed: 26846640]

[22]. Kalsotra A, Xiao X, Ward AJ, Castle JC, Johnson JM, Burge CB, Cooper TA, A postnatal switch of CELF and MBNL proteins reprograms alternative splicing in the developing heart, Proceedings of the National Academy of Sciences of the United States of America 105(51) (2008) 20333–8. [PubMed: 19075228]

[23]. Zhang J, Bahi N, Llovera M, Comella JX, Sanchis D, Polypyrimidine tract binding proteins (PTB) regulate the expression of apoptotic genes and susceptibility to caspase-dependent apoptosis in differentiating cardiomyocytes, Cell Death Differ 16(11) (2009) 1460–8. [PubMed: 19590510]

[24]. Verma SK, Deshmukh V, Liu P, Nutter CA, Espejo R, Hung ML, Wang GS, Yeo GW, Kuyumcu-Martinez MN, Reactivation of fetal splicing programs in diabetic hearts is mediated by protein kinase C signaling, J Biol Chem 288(49) (2013) 35372–86. [PubMed: 24151077]

[25]. Bland CS, Cooper TA, Micromanaging alternative splicing during muscle differentiation, Developmental cell 12(2) (2007) 171–2. [PubMed: 17276332]

[26]. Gueroussov S, Gonatopoulos-Pournatzis T, Irimia M, Raj B, Lin ZY, Gingras AC, Blencowe BJ, An alternative splicing event amplifies evolutionary differences between vertebrates, Science 349(6250) (2015) 868–73. [PubMed: 26293963]

[27]. Homsy J, Zaidi S, Shen Y, Ware JS, Samocha KE, Karczewski KJ, DePalma SR, McKean D, Wakimoto H, Gorham J, Jin SC, Deanfield J, Giardini A, Porter GA Jr., Kim R, Bilguvar K, Lopez-Giraldez F, Tikhonova I, Mane S, Romano-Adesman A, Qi H, Vardarajan B, Ma L, Daly M, Roberts AE, Russell MW, Mital S, Newburger JW, Gaynor JW, Breitbart RE, Iossifov I, Ronemus M, Sanders SJ, Kaltman JR, Seidman JG, Brueckner M, Gelb BD, Goldmuntz E, Lifton RP, Seidman CE, Chung WK, De novo mutations in congenital heart disease with neurodevelopmental and other congenital anomalies, Science 350(6265) (2015) 1262–6. [PubMed: 26785492]

[28]. Wei C, Qiu J, Zhou Y, Xue Y, Hu J, Ouyang K, Banerjee I, Zhang C, Chen B, Li H, Chen J, Song LS, Fu XD, Repression of the central splicing regulator RBFox2 is functionally linked to pressure overload-induced heart failure, Cell Rep 10 (2015) 1521–1533. [PubMed: 25753418]

[29]. Nutter CA, Jaworski EA, Verma SK, Deshmukh V, Wang Q, Botvinnik OB, Lozano MJ, Abass IJ, Ijaz T, Brasier AR, Garg NJ, Wehrens XH, Yeo GW, Kuyumcu-Martinez MN, Dysregulation of RBFOX2 Is an early event in cardiac pathogenesis of diabetes, Cell Rep 15(10) (2016) 2200–13. [PubMed: 27239029]

[30]. Garg NJ, Bhatia V, Gerstner A, deFord J, Papaconstantinou J, Gene expression analysis in mitochondria from Chagas mice: Alterations in specific metabolic pathways, Biochemical J. 381 (2004) 743–752.

[31]. Dhiman M, Coronado YA, Vallejo CK, Petersen JR, Ejilemele A, Nunez S, Zago MP, Spratt HM, Garg NJ, Innate immune responses and antioxidant/oxidant imbalance are major determinants of human Chagas disease., Plos NTD 7(8) (2013) e2364.

[32]. Wan X-X, Gupta S, Zago MP, Davidson MM, Dousset P, Amoroso A, Garg NJ, Defects of mtDNA replication impaired the mitochondrial biogenesis during *Trypanosoma cruzi* infection in human cardiomyocytes and Chagas patients: The role of Nrf1/2 and antioxidant response, J Am Heart Assoc 1(6) (2012) e003855 [PubMed: 23316324]

[33]. Wen JJ, Yin YW, Garg NJ, PARP1 depletion improves mitochondrial and heart function in Chagas disease: Effects on POLG dependent mtDNA maintenance, PLoS Pathog 14(5) (2018) e1007065. [PubMed: 29851986]

[34]. Wen J-J, Bhatia V, Popov VL, Garg NJ, Phenyl-alpha-tert-butyl nitrone reverses mitochondrial decay in acute Chagas disease, Am J Pathol 169(6) (2006) 1953–64. [PubMed: 17148660]

[35]. Dobin A, Davis CA, Schlesinger F, Drenkow J, Zaleski C, Jha S, Batut P, Chaisson M, Gingeras TR, STAR: Ultrafast universal RNA-seq aligner, Bioinformatics 29(1) (2013) 15–21. [PubMed: 23104886]

[36]. Liao Y, Smyth GK, Shi W, FeatureCounts: an efficient general purpose program for assigning sequence reads to genomic features, Bioinformatics 30(7) (2014) 923–30. [PubMed: 24227677]

[37]. Love MI, Huber W, Anders S, Moderated estimation of fold change and dispersion for RNA-seq data with DESeq2, Genome Biol 15(12) (2014) 550. [PubMed: 25516281]

[38]. Katz Y, Wang ET, Airoldi EM, Burge CB, Analysis and design of RNA sequencing experiments for identifying isoform regulation, Nat Methods 7(12) (2010) 1009–15. [PubMed: 21057496]

[39]. Koo SJ, Spratt HM, Soman KV, Stafford S, Gupta S, Petersen JR, Zago MP, Martinez MN, Brasier AR, Wiktorowicz JE, Garg NJ, S-Nitrosylation proteome profile of peripheral blood mononuclear cells in human heart failure, Int J Proteomics 2016 (2016) 1384523. [PubMed: 27635260]

[40]. Garg NJ, Soman KV, Zago MP, Koo SJ, Spratt H, Stafford S, Blell ZN, Gupta S, Nunez Burgos J, Barrientos N, Brasier AR, Wiktorowicz JE, Changes in proteome profile of peripheral blood mononuclear cells in chronic Chagas disease, PLoS Negl Trop Dis 10(2) (2016) e0004490. [PubMed: 26919708]

[41]. Wan X, Wen JJ, Koo SJ, Liang LY, Garg NJ, SIRT1-PGC1alpha-NFkappaB Pathway of oxidative and inflammatory stress during *Trypanosoma cruzi* infection: Benefits of SIRT1-targeted therapy in improving heart function in Chagas disease, PLoS Pathog 12(10) (2016) e1005954. [PubMed: 27764247]

[42]. Nutter CA, Kuyumcu-Martinez MN, Emerging roles of RNA-binding proteins in diabetes and their therapeutic potential in diabetic complications, Wiley Interdiscip Rev RNA 9(2) (2018).

[43]. Yeo GW, Coufal NG, Liang TY, Peng GE, Fu XD, Gage FH, An RNA code for the FOX2 splicing regulator revealed by mapping RNA-protein interactions in stem cells, Nat Struct Mol Biol 16(2) (2009) 130–7. [PubMed: 19136955]

[44]. Dufurrena Q, Amjad FM, Scherer PE, Weiss LM, Nagajyothi J, Roth J, Tanowitz HB, Kuliawat R, Alterations in pancreatic beta cell function and *Trypanosoma cruzi* infection: evidence from human and animal studies, Parasitol Res 116(3) (2017) 827–838. [PubMed: 28013375]

[45]. Layland J, Li JM, Shah AM, Role of cyclic GMP-dependent protein kinase in the contractile response to exogenous nitric oxide in rat cardiac myocytes, J Physiol 540(Pt 2) (2002) 457–67. [PubMed: 11956336]

[46]. Takimoto E, Cyclic GMP-dependent signaling in cardiac myocytes, Circ J 76(8) (2012) 1819–25. [PubMed: 22785374]

[47]. Zhang M, Kass DA, Phosphodiesterases and cardiac cGMP: evolving roles and controversies, Trends Pharmacol Sci 32(6) (2011) 360–5. [PubMed: 21477871]

[48]. Lee DI, Kass DA, Phosphodiesterases and cyclic GMP regulation in heart muscle, Physiology (Bethesda) 27(4) (2012) 248–58. [PubMed: 22875455]

[49]. Nagayama T, Zhang M, Hsu S, Takimoto E, Kass DA, Sustained soluble guanylate cyclase stimulation offsets nitric-oxide synthase inhibition to restore acute cardiac modulation by sildenafil, J Pharmacol Exp Ther 326(2) (2008) 380–7. [PubMed: 18456872]

[50]. Seya K, Ono K, Fujisawa S, Okumura K, Motomura S, Furukawa K, Cytosolic Ca2+-induced apoptosis in rat cardiomyocytes via mitochondrial NO-cGMP-protein kinase G pathway, J Pharmacol Exp Ther 344(1) (2013) 77–84. [PubMed: 23104881]

[51]. Verma SK, Deshmukh V, Nutter CA, Jaworski E, Jin W, Wadhwa L, Abata J, Ricci M, Lincoln J, Martin JF, Yeo GW, Kuyumcu-Martinez MN, Rbfox2 function in RNA metabolism is impaired in hypoplastic left heart syndrome patient hearts, Sci Rep 6 (2016) 30896. [PubMed: 27485310]

[52]. Bonney KM, Luthringer DJ, Kim SA, Garg NJ, Engman DM, Pathology and Pathogenesis of Chagas heart disease., Annual Review Pathol 14 (2019) 421–447.

[53]. Glover TL, Galvan E, Diabetes and heart failure, Crit Care Nurs Clin North Am 25(1) (2013) 93–9. [PubMed: 23410648]

[54]. Qian L, Hong J, Zhang Y, Zhu M, Wang X, Zhang Y, Chu M, Yao J, Xu D, Downregulation of S100A4 alleviates cardiac fibrosis via wnt/beta-catenin pathway in mice, Cell Physiol Biochem 46(6) (2018) 2551–2560. [PubMed: 29758552]

[55]. Fu S, Ping P, Wang F, Luo L, Synthesis, secretion, function, metabolism and application of natriuretic peptides in heart failure, J Biol Eng 12 (2018) 2. [PubMed: 29344085]

[56]. Nutter CA, Jaworski E, Verma SK, Perez-Carrasco Y, Kuyumcu-Martinez MN, Developmentally regulated alternative splicing is perturbed in type 1 diabetic skeletal muscle, Muscle Nerve 56(4) (2017) 744–749. [PubMed: 28164326]

[57]. Padanyi R, Paszty K, Hegedus L, Varga K, Papp B, Penniston JT, Enyedi A, Multifaceted plasma membrane Ca(2+) pumps: From structure to intracellular Ca(2+) handling and cancer, Biochim Biophys Acta 1863(6) (2016) 1351–63. [PubMed: 26707182]

[58]. Penniston JT, Padanyi R, Paszty K, Varga K, Hegedus L, Enyedi A, Apart from its known function, the plasma membrane Ca(2)(+)ATPase can regulate Ca(2)(+) signaling by controlling phosphatidylinositol 4,5-bisphosphate levels, J Cell Sci 127(Pt 1) (2014) 72–84. [PubMed: 24198396]

[59]. Tabara Y, Kohara K, Kita Y, Hirawa N, Katsuya T, Ohkubo T, Hiura Y, Tajima A, Morisaki T, Miyata T, Nakayama T, Takashima N, Nakura J, Kawamoto R, Takahashi N, Hata A, Soma M, Imai Y, Kokubo Y, Okamura T, Tomoike H, Iwai N, Ogihara T, Inoue I, Tokunaga K, Johnson T, Caulfield M, Munroe P, C. Global Blood Pressure Genetics, Umemura S, Ueshima H, Miki T, Common variants in the ATP2B1 gene are associated with susceptibility to hypertension: the Japanese Millennium Genome Project, Hypertension 56(5) (2010) 973–80. [PubMed: 20921432]

[60]. Little R, Zi M, Hammad SK, Nguyen L, Njegic A, Kurusamy S, Prehar S, Armesilla AL, Neyses L, Austin C, Cartwright EJ, Reduced expression of PMCA1 is associated with increased blood pressure with age which is preceded by remodelling of resistance arteries, Aging Cell 16(5) (2017) 1104–1113. [PubMed: 28795531]

[61]. Creemers EE, Sutherland LB, McAnally J, Richardson JA, Olson EN, Myocardin is a direct transcriptional target of Mef2, Tead and Foxo proteins during cardiovascular development, Development 133(21) (2006) 4245–56. [PubMed: 17021041]

[62]. Desjardins CA, Naya FJ, The function of the MEF2 family of transcription factors in cardiac development, cardiogenomics, and direct reprogramming, J Cardiovasc Dev Dis 3(3) (2016).

[63]. Naya FJ, Black BL, Wu H, Bassel-Duby R, Richardson JA, Hill JA, Olson EN, Mitochondrial deficiency and cardiac sudden death in mice lacking the MEF2A transcription factor, Nat Med 8(11) (2002) 1303–9. [PubMed: 12379849]

[64]. Chen X, Gao B, Ponnusamy M, Lin Z, Liu J, MEF2 signaling and human diseases, Oncotarget 8(67) (2017) 112152–112165. [PubMed: 29340119]

[65]. Estrella NL, Clark AL, Desjardins CA, Nocco SE, Naya FJ, MEF2D deficiency in neonatal cardiomyocytes triggers cell cycle re-entry and programmed cell death in vitro, J Biol Chem 290(40) (2015) 24367–80. [PubMed: 26294766]

[66]. Zhu B, Gulick T, Phosphorylation and alternative pre-mRNA splicing converge to regulate myocyte enhancer factor 2C activity, Mol Cell Biol 24(18) (2004) 8264–75. [PubMed: 15340086]

[67]. Litosch I, Novel mechanisms for feedback regulation of phospholipase C-beta activity, IUBMB Life 54(5) (2002) 253–60. [PubMed: 12587975]

[68]. Cocco L, Follo MY, Manzoli L, Suh PG, Phosphoinositide-specific phospholipase C in health and disease, J Lipid Res 56(10) (2015) 1853–60. [PubMed: 25821234]

[69]. Jalili T, Takeishi Y, Walsh RA, Signal transduction during cardiac hypertrophy: the role of G alpha q, PLC beta I, and PKC, Cardiovasc Res 44(1) (1999) 5–9. [PubMed: 10615383]

[70]. Wang D, Papp AC, Binkley PF, Johnson JA, Sadee W, Highly variable mRNA expression and splicing of L-type voltage-dependent calcium channel alpha subunit 1C in human heart tissues, Pharmacogenet Genomics 16(10) (2006) 735–45. [PubMed: 17001293]

[71]. Lu Z, Jiang YP, Xu XH, Ballou LM, Cohen IS, Lin RZ, Decreased L-type Ca2+ current in cardiac myocytes of type 1 diabetic Akita mice due to reduced phosphatidylinositol 3-kinase signaling, Diabetes 56(11) (2007) 2780–9. [PubMed: 17666471]

[72]. Russwurm C, Zoidl G, Koesling D, Russwurm M, Dual acylation of PDE2A splice variant 3: targeting to synaptic membranes, J Biol Chem 284(38) (2009) 25782–90. [PubMed: 19632989]

[73]. Cabalen ME, Cabral MF, Sanmarco LM, Andrada MC, Onofrio LI, Ponce NE, Aoki MP, Gea S, Cano RC, Chronic *Trypanosoma cruzi* infection potentiates adipose tissue macrophage polarization toward an anti-inflammatory M2 phenotype and contributes to diabetes progression in a diet-induced obesity model, Oncotarget 7(12) (2016) 13400–15. [PubMed: 26921251]

[74]. Nagajyothi F, Desruisseaux MS, Weiss LM, Chua S, Albanese C, Machado FS, Esper L, Lisanti MP, Teixeira MM, Scherer PE, Tanowitz HB, Chagas disease, adipose tissue and the metabolic syndrome, Mem Inst Oswaldo Cruz 104 Suppl 1 (2009) 219–25. [PubMed: 19753477]

[75]. Jackson Y, Castillo S, Hammond P, Besson M, Brawand-Bron A, Urzola D, Gaspoz JM, Chappuis F, Metabolic, mental health, behavioural and socioeconomic characteristics of migrants with Chagas disease in a non-endemic country, Trop Med Int Health 17(5) (2012) 595–603. [PubMed: 22487303]

[76]. Nagajyothi F, Desruisseaux MS, Machado FS, Upadhya R, Zhao D, Schwartz GJ, Teixeira MM, Albanese C, Lisanti MP, Chua SC Jr., Weiss LM, Scherer PE, Tanowitz HB, Response of adipose tissue to early infection with *Trypanosoma cruzi* (Brazil strain), J Infect Dis 205(5) (2012) 830–40. [PubMed: 22293433]

[77]. dos Santos VM, da Cunha SF, Teixeira Vde P, Monteiro JP, dos Santos JA, dos Santos TA, dos Santos LA, da Cunha DF, Frequency of diabetes mellitus and hyperglycemia in chagasic and non-chagasic women, Rev Soc Bras Med Trop 32(5) (1999) 489–96. [PubMed: 10881081]

Highlights

- Diabetes is on the rise in Chagas disease (ChD) patients.
- Aberrations of the cGMP-PKG-Ca^{2+} pathway are implicated in cardiovascular complications of diverse etiologies.
- Changes in expression of 26 genes associated with mobilization and cellular levels of Ca^{2+} occurred in ChD hearts.
- RBFOX (RNA binding protein)-dependent differential splicing of 11 genes of the cGMP-PKG pathway occurred in ChD and/or diabetic hearts.
- Alternative splicing-mediated dysregulation of critical genes associated with myocardial cGMP-PKG-Ca^{2+} signaling may exacerbate the cardiac disease severity in ChD presented with diabetes.

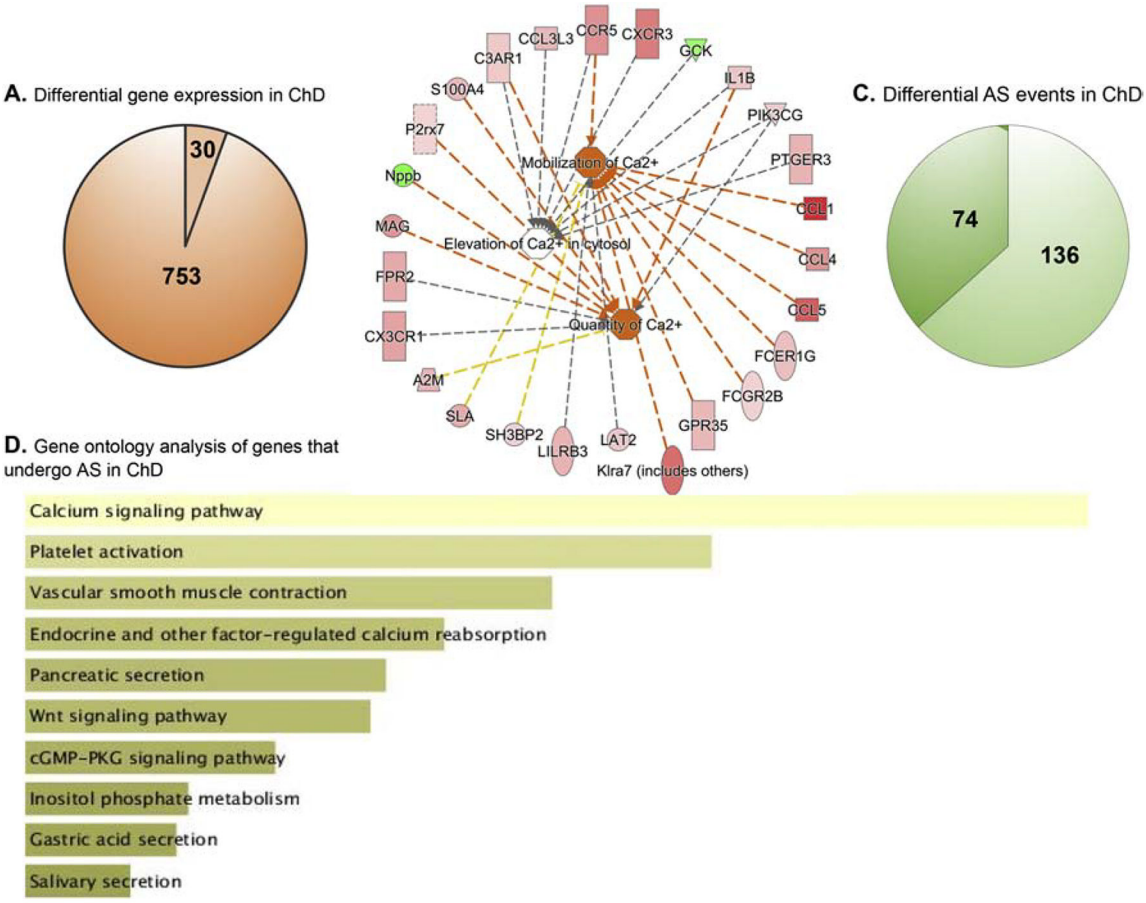

Figure 1: Global changes in gene expression and alternative splicing in chronic Chagas disease mouse hearts.

C57BL/6 female mice were infected with *Trypanosoma cruzi* (10,000 parasites per mouse). Mice were euthanized at 150 days' post-infection corresponding to chronic Chagas disease (ChD) phase. Total RNA was isolated from heart tissues of normal and ChD mice ($n \geq 3$ mice per group) and high throughput sequencing was performed. After normalizing, datasets were analyzed to identify the global changes in gene expression and alternative splicing (AS) of genes as described in Materials and Methods. **(A)** Venn diagram shows global changes in gene expression in ChD (vs. normal controls) mice (fold change $|\geq 1.2|$, p value ≤ 0.01, up regulated: 753 genes, down regulated: 30 genes. The transcriptome data are presented in Table S2. **(B)** Ingenuity Pathway Analysis of the differential transcriptome dataset was performed to develop the network of Ca^{2+} mobilization and cellular homeostasis in ChD (vs. control) murine hearts. In the network, the intensity of pink/red and green colors show the extent of increase and decrease in gene expression, respectively, in ChD vs. control murine hearts. Brownish orange node/lines show predicted activation of the pathway. Gray and yellow lines are used when putative effect is not completely understood. **(C)** Venn diagram shows the distribution of cassette exon exclusion (74/210, 35%) and exon inclusion (136/210, 65%) in ChD (vs. control) mouse hearts ($p<0.01$). The list of genes that undergo AS in ChD (vs. control) hearts is presented in Table S3. **(D)** Top significant gene ontology and pathway analysis of alternatively spliced genes in the myocardium of ChD (vs. control)

mice. Enrichr server and KEGG 2019 mouse pathway analysis were used to categorize AS genes based on their roles in signaling pathways.

Figure 2: Alternative splicing of genes involved in the cGMP-PKG-Ca^{2+} signaling pathway(s) in ChD mice.

Shown are the representative genome browser images of AS of genes of the cGMP-PKG-Ca^{2+} pathway in ChD mice. Data show annotation of the findings based on RNA-Seq reads in ChD murine hearts in comparison to that noted in control mice. **(A)** *Atp2b1* exon 5, **(B)** *Atp2b1* exon 21, **(C)** *Mef2a* exon 9, **(D)** *Atp2a3* exon 21, **(E)** *Arhgef10* Exon 9, and **(F)** *Plcb1* exon 32. In each panel, data from control mice are presented below the data from ChD murine hearts.

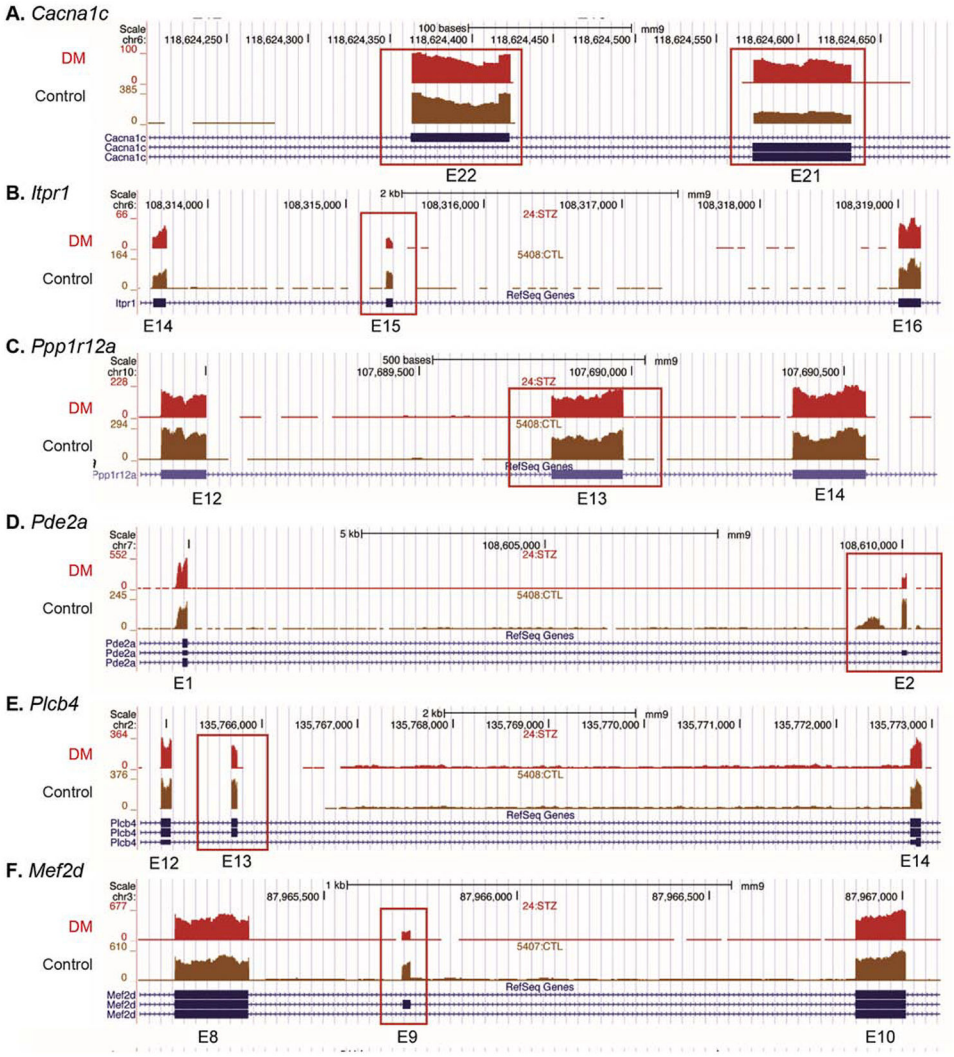

Figure 3: AS pattern of genes involved in the cGMP-PKG-Ca^{2+} pathway in diabetic mouse heart.

Shown are representative genome browser images depicting alternative splicing of **(A)** *Cacna1c* exon 21 and 22, **(B)** *Itpr1* exon 15, **(C)** *ppp1r12a* exon 13, **(D)** *Pde2a* exon 2, **(E)** *Plcb4* exon 13, and **(F)** *Mef2d* exon 9 in DM murine hearts. These genes were identified to be alternatively spliced based on MISO analysis of the RNA-Seq dataset in DM mouse left ventricles (vs. controls, n ≥ 3 mice per group). The RNA-Seq dataset is available at [29].

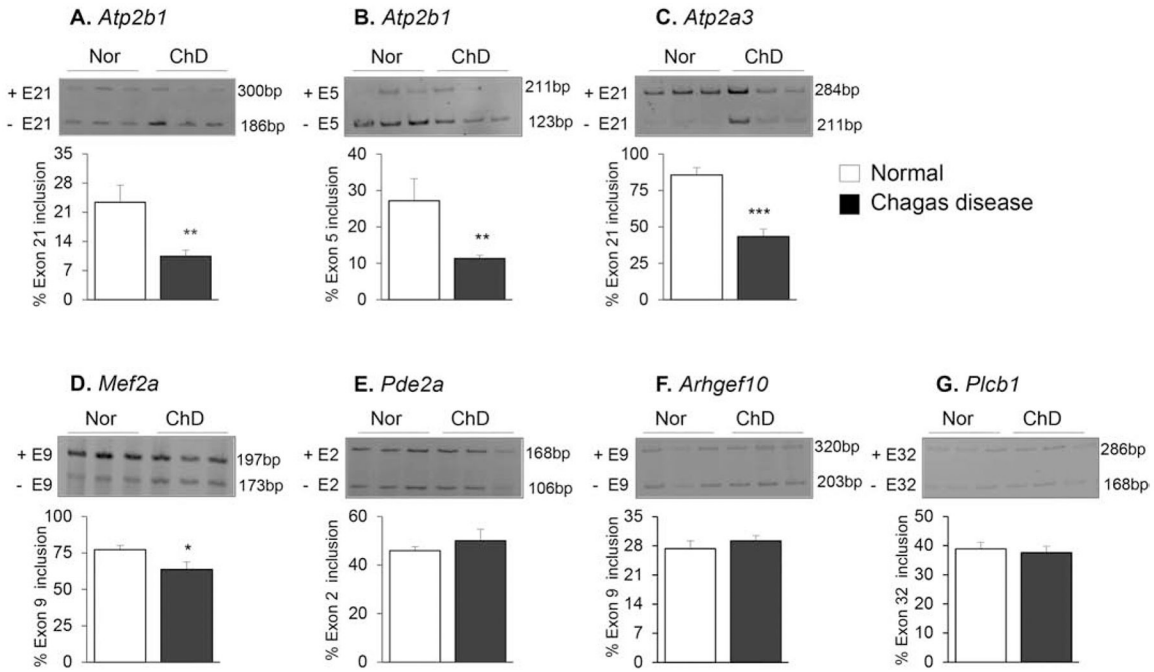

Figure 4: Validation of differential AS of genes of the cGMP-PKG-Ca^{2+} pathway in ChD mice.

Total RNA was isolated from heart tissue of normal and ChD mice. Semi-quantitative RT-PCR was performed as described in Materials and Methods to examine the inclusion and exclusion of specified exons. **(A)** *Atp2b1* exon 21, **(B)** *Atp2b1* exon 5, **(C)** *Atp2a3* exon 21, **(D)** *Mef2a* exon 9, **(E)** *Pde2a* exon 2, **(F)** *Arhgef10* exon 9, and **(G)** *Plcb1* exon 32. The representative images of AS gels are shown in top panels (+ E = Exon inclusion and − E = Exon exclusion). The bottom panels show the percentage changes in inclusion of specified exons. Data in bar graphs are representative of two independent experiments (n = 3 mice per group per experiment), and are presented as mean value ± SD. The unpaired *t* test was used to calculate statistically significant differences between two sample groups, and presented as *p ≤ 0.05, **p ≤ 0.01, or ***p ≤ 0.001 (ChD vs. normal).

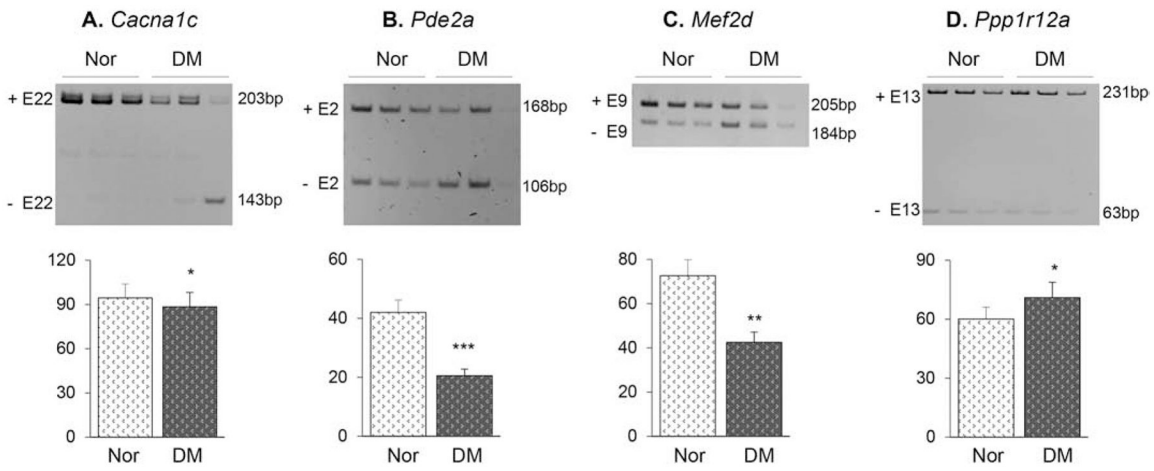

Figure 5. Validation of differential alternative splicing of cGMP-PKG-Ca^{2+} pathway genes in diabetic mice.

Total RNA was obtained from heart tissue of DM and normal control mice. Semi-quantitative RT-PCR was performed to examine the inclusion and exclusion of specified exons. **(A)** exon 22 in *Cacna1c*, **(B)** exon 2 in *Pde2a*, **(C)** exon 9 in *Mef2d*, and **(D)** exon 13 in *Ppp1r12a*. The representative images of AS gels are shown in top panels (+ E = Exon inclusion and − E = Exon exclusion). The bottom panels show the percentage changes in inclusion of specified exons and are representative of two independent experiments (n=3 mice per group per experiment). Data are presented as mean value ± SD. The unpaired *t* test was used to calculate statistically significant differences between two sample groups, and plotted as *$p \leq 0.05$, **$p \leq 0.01$, or *** $p \leq 0.001$ (diabetic vs. normal controls).

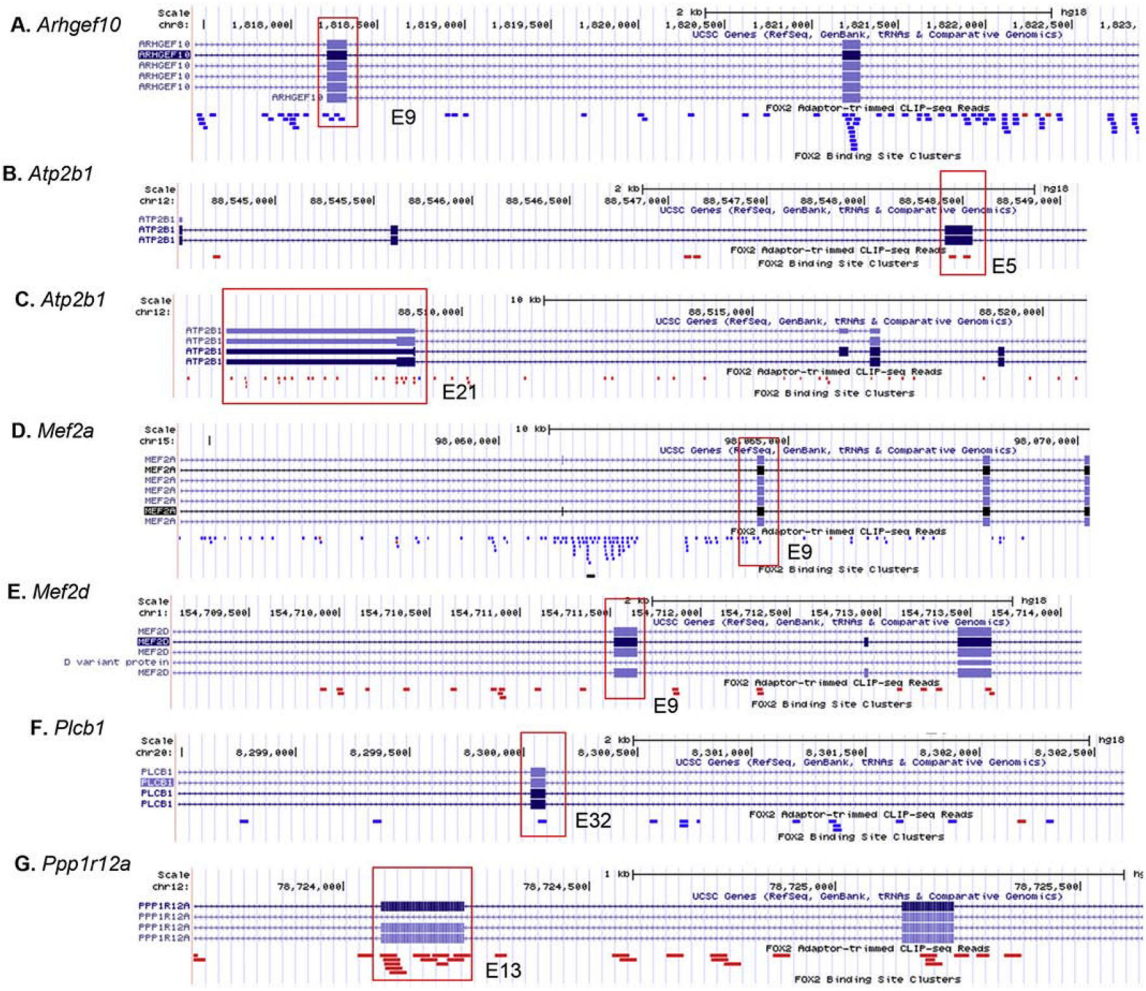

Figure 6. Presence of RBFOX2-binding sites in genes of the cGMP-PKG-Ca^{2+} signaling pathway.

Publicly available human CLIP-Seq dataset were used to identify the RBFOX2-binding motifs within genes of the cGMP-PKG-Ca^{2+} signaling pathway. Shown are the genome browser images of genes of the cGMP-PKG-Ca^{2+} pathway that consisted RBFOX2-binding sites. These included **(A)** *Arhgef10*, **(B & C)** *Atp2b1*, **(D)** *Mef2a*, **(E)** *Mef2d*, **(F)** *Plcb1*, and **(G)** *Ppp1r12a*. The RBFOX2-binding clusters are shown in blue dots (positive strand) and red dots (negative strand). The specific exons that were identified to be mis-spliced in each gene are marked by a red box and exon number.

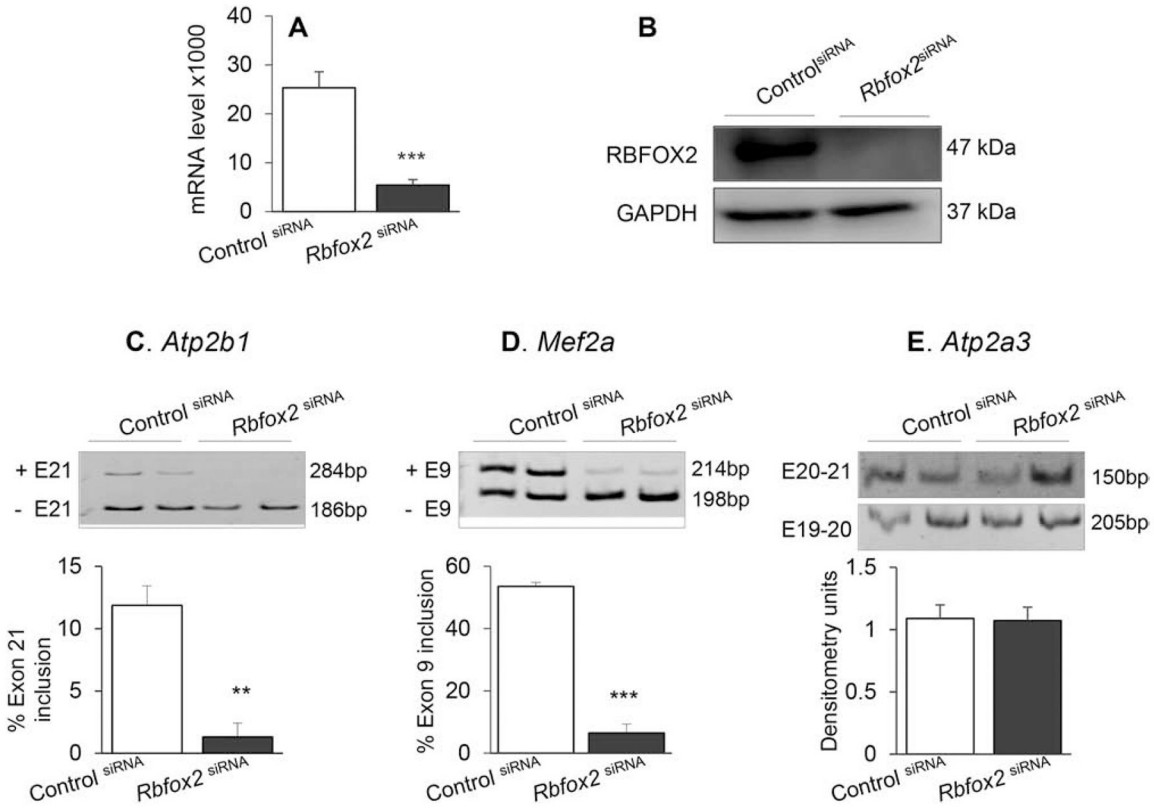

Figure 7. RBFOX2 regulates AS in genes of the cGMP-PKG-Ca^{2+} signaling pathway.

H9c2 cells were transfected with *Rbfox2* siRNA (targets exon 6) or scrambled control siRNA as described in Materials and Methods. **(A)** Total RNA was isolated from transfected cells, and *Rbfox2* and *Gapdh* (control) mRNA levels were determined by real time RT-qPCR. Bar graph shows *Rbfox2* mRNA level, normalized to *Gapdh* mRNA level, in transfected cells. **(B)** Total protein lysates from siRNA-treated H9c2 cells were analyzed by Western blotting by using an antibody against RBFOX2 to determine the depletion efficiency of *Rbfox2* siRNA. Western blotting for GAPDH was performed to confirm equal protein loading. **(C-E)** Total RNA was isolated from H9c2 cells transfected with scrambled (control) or *Rbfox2*-specific siRNAs, and exclusion/inclusion assay was performed as described in Materials and Methods to determine the RBFOX2-dependent inclusion of specific exons. Shown are representative images (top panels) for alternative splicing in **(C)** *Atp2b1* exon 21, **(D)** *Mef2a* exon 9, and **(E)** *Atp2a3* exons 20–21 and exons 19–20 (+ E and −E indicate the inclusion and exclusion of the specific exon, respectively). The bar graphs below the gel images show the percentage changes in inclusion of specified exons. Data in bar graphs are representative of three independent experiments (duplicate observations per experiment per sample), and presented as mean value ± SD. The unpaired *t* test was used to calculate statistically significant differences between two sample groups and presented as $^{**}p < 0.01$ and $^{***}p < 0.001$ (*Rbfox2* siRNA vs. control siRNA).

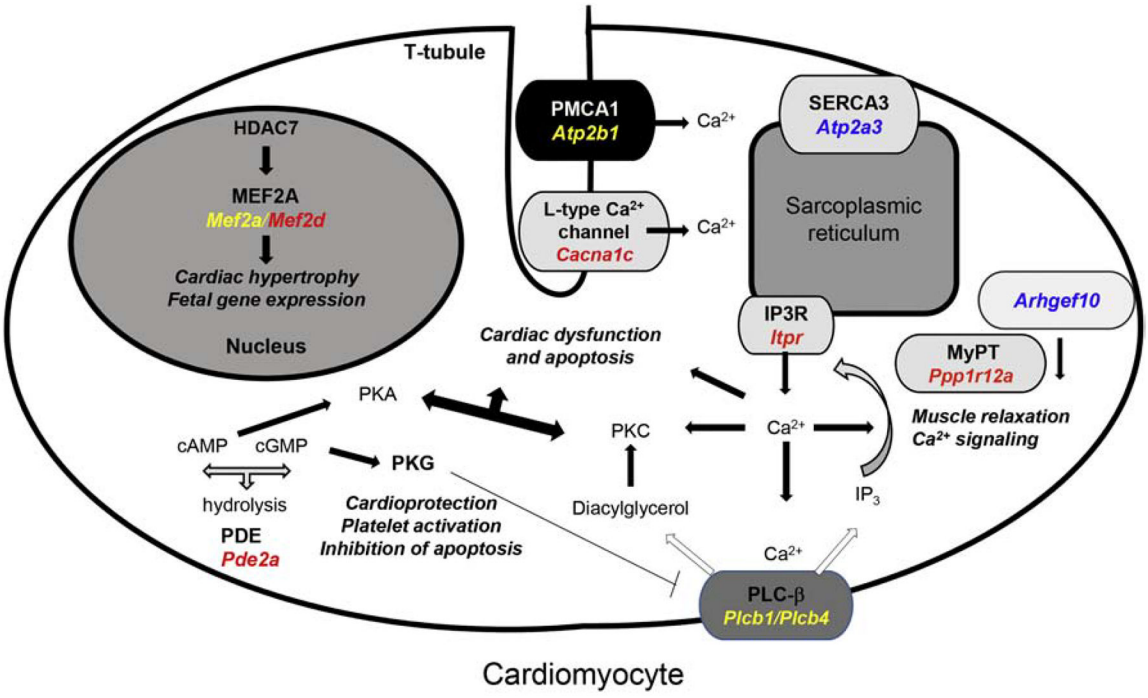

Figure 8. The genes within the cGMP-PKG-Ca^{2+} signaling pathway altered via alternative splicing in the myocardium of DM and ChD mice.

Schematic representation of processes and cGMP-PKG-Ca^{2+} signaling cascades affected via AS in the heart under ChD and diabetic conditions are shown. The genes that were identified to be alternatively spliced and encode for proteins involved in Ca^{2+} flux, Ca^{2+} signaling and contractile activity are shown in bold/italics font. Genes of the signaling cascade identified to be affected via alternative splicing under diabetic conditions are labeled in red, in ChD hearts in blue, and common in both diseases in yellow color. Please see Table 1 for gene/protein names, molecular functional details, and summarized results. Briefly, in the heart, cGMP is activated by nitric oxide and natriuretic peptides and its downstream effects are mediated by cGMP-dependent protein kinase (PKG). PKG phosphorylates several proteins including PLC-beta and plays an essential role in regulation of Ca^{2+} signaling and contraction and relaxation of cardiac myocytes. For example, PKG/PLC-β influence the function of plasma membrane Ca^{2+} ATPase (PMCA1), L-type Ca^{2+} channel (CACNA1C), Inositol trisphosphate receptor (IP3R), and SERCA3 that together determine the intracellular calcium homeostasis during muscle excitation, contraction and relaxation. Genes encoding for calcium sensing Rho guanine nucleotide exchange factor 10 (Arhgef10) and myosin phosphatase (MyPT) that regulate actin-myosin interaction were also impacted by alternative splicing in ChD and/or DM heart. Phosphodiesterases (PDE2, PDE3) catabolize the cGMP/cAMP and inhibit PKG activation.

We have found that AS changes in the genes of the cGMP-PKG-Ca^{2+} signaling pathway in ChD and DM hearts. *Atp2b1*, and *Mef2a* were similarly mis-spliced in both ChD and DM hearts and were regulated by RBFOX2. *Cacna1c*, *Itpr*, *Ppp1r12a* were differentially spliced in the heart of diabetic mice; and *Arhgef10* and *Atp2a3* were differentially spliced in the heart of ChD mice. The AS events can impact the function of the target genes [20, 21] and *T. cruzi* infection is linked to increased risk of DM in Chagas patients (reviewed in [44]). We

propose that DM can potentially exacerbate the AS-induced dysregulation of cGMP-PKG-Ca^{2+} pathway and the severity of cardiomyopathy and heart failure in Chagas disease.

Table 1.

Genes of the cGMP-dependent Protein Kinase G (PKG) / Ca^{2+} signaling pathway that were identified to be alternatively spliced by RNA-Seq/MISO analysis in ChD and/or T1D murine hearts.

Gene name	Protein	Molecular function	AS by RNA-Seq		AS by RTPCR		RBFOX2 CLIP Seq
			ChD	DM	ChD	DM	
Arhgef10	Ca^{2+} sensing Rho guanine nucleotide exchange factor 10 (also called Rho-GEF)	Stimulates exchange of GDP for GTP and regulates the activity of small Rho GTPases	√				√
Atp2b1	Plasma membrane Ca^{2+} transporting ATPase 1 (PMCA1)	Removes intracellular Ca^{2+} and maintains intracellular calcium homeostasis	√	√	√	√	√
Atp2a3	ATPase sarcoplasmic/endoplasmic reticulum (SR) Ca^{2+} transporting 3 (also called SERCA3)	Catalyzes ATP-dependent sequestration of Ca^{2+} in SR with muscle excitation and contraction	√		√		
Cacna1c	Calcium voltage-gated channel subunit α-1C (component of L-type voltage -d- Ca^{2+} channel)	Mediates Ca^{2+} influx upon membrane polarization with muscle excitation-contraction in the heart		√			
Itpr1	Inositol 1,4,5-trisphosphate (IP3) receptor type 1	Intracellular IP3-stimulated receptor, modulates Ca^{2+} release from ER		√			
Mef2a	Myocyte enhancer factor 2A (Ca^{2+}-sensitive transcription factor)	Activates muscle-specific, growth factor- and stress-induced genes.	√	√	√	√	√
Mef2d	Myocyte enhancer factor 2D	Regulated by class II HDACs, controls muscle and neuronal cell differentiation and development		√		√	√
Plcb1	Phospholipase C beta (phosphatidylinositol 4,5-bisphosphate → inositol 1,4,5-triphosphate and diacylglycerol)	Regulation of G-protein mediated intracellular Ca^{2+} level by NO-cGMP-PKG signaling pathway	√				√
Plcb4	Phospholipase C beta isoform	As above		√			
Pde2a	Phosphodiesterase 2A (catalyzes hydrolysis of cAMP and cGMP)	Provides feedback control of PKG-protein kinase A activities			√	√	
Ppp1r12a (Mypt)	Protein phosphatase 1 regulatory subunit 12A (subunit of myosin phosphatase)	Regulates actin-myosin interaction downstream of GTP-RhoA, role in smooth muscle contraction		√		√	√

Listed are the genes of cGMP-PKG-Ca^{+2} signaling pathway that were studied for alternative splicing (AS) in the myocardium of murine models of diabetes and Chagas disease (ChD) in comparison to matched controls.